

Study on the effect of different types of sugar on lipid deposition in goose fatty liver

Rongxue Wei,^{*,1} Donghang Deng,^{*,1} Yongqiang Teng,^{*} Cancang Lu,^{*} Zhaoyun Luo,^{*} Mariama Abdulai,^{*} Hehe Liu,^{*} Hongyong Xu,^{*} Liang Li,^{*} Shenqiang Hu,^{*} Jiwei Hu,^{*} Shouhai Wei,[†] Xianyin Zeng,[†] and Chunchun Han ^{*,2}

^{*}*Farm Animal Genetic Resources Exploration and Innovation Key Laboratory of Sichuan Province, Sichuan Agricultural University, Chengdu, Sichuan, 611130, P.R. China; and* [†]*College of Life Science, Sichuan Agricultural University, Ya'an, Sichuan, 625014, P.R. China*

ABSTRACT Early research in our lab indicated that the effect of glucose, fructose and sucrose on the levels of triacylglycerol, and inflammatory factor was significantly different, and it is speculated that the regulatory mechanism of lipid deposition by different type of sugar in the liver is different. In order to explore lipid deposition difference mediated by different types of sugar (glucose, fructose, and sucrose) in goose fatty liver formation, this experiment was performed from cell culture, overfeeding experiment, and transcriptome analysis at 3 levels. Cell culture experiment results indicated that the levels of intracellular triglyceride, total cholesterol, and lipid content of fructose and sucrose treatment were significantly higher than those of glucose treatment ($P < 0.05$). In slaughter performance, the liver weight,

the ratio of liver weight to body weight, feed conversion ratio (liver weight/feed consumption) were better in sucrose overfeeding group ($P < 0.05$). In addition, the liver of the sucrose overfeeding group contained a lot of unsaturated fatty acids, especially (n-3) polyunsaturated fatty acids ($P < 0.05$). Transcriptome analysis shown that the peroxisome proliferators-activated receptor (**PPAR**) signaling pathway is highly enriched in the fructose and sucrose overfeeding groups; cell cycle, and DNA replication pathways were highly enriched in the glucose overfeeding group. In conclusion, due to the decrease of lipids outward transportation and the anti-inflammation of unsaturated fatty acids, fructose, and sucrose have better ability to induce steatosis in goose fatty liver formation.

Key words: goose fatty liver, glucose, fructose, sucrose, lipid deposition

2022 Poultry Science 101:101729
<https://doi.org/10.1016/j.psj.2022.101729>

INTRODUCTION

The metabolic responses to different types of sugar overintake varied from study to study. Studies have shown that people who consume fructose have higher levels of triacylglycerol (**TG**) than those who consume the same amount of glucose (Kawasaki et al., 2009). Studies have shown that there is a gap in acute metabolism between high fructose corn syrup and sucrose. After consuming the same amount of high fructose syrup, blood fructose concentration was higher than that of sucrose, thus resulting in a higher blood sugar value in the body. As for the reason, the explanation of this study is that the

glucose component in sucrose can inhibit the activity of sucrase, affecting the hydrolysis of sucrose, and resulting in lower fructose content (Le et al., 2012). Compared with the fructose and glucose treatment, the rats fed the fructose diet had higher body weight and food intake, especially during the immature period (Le et al., 2012). The result suggested that fructose cause a higher intake than glucose, thereby increasing the possibility of other diseases. In conclusion, there is still a great debate on the metabolic differences caused by different types of sugar excessive intake. Moreover, it is still in the preliminary stage of research and has been seldom reported.

As a powerful synthetic and catabolic organ, an important metabolic function of the liver is to maintain the steady state of plasma glucose concentration under any nutritional state of the body. When energy is excess, the excess glucose can be converted into lipids and stored in the liver through fatty acid de novo synthesis. Under normal basic physiological conditions, only 5% of lipids in the liver are derived from the de novo synthesis pathway of endogenous lipids. However, in pathological

© 2022 The Authors. Published by Elsevier Inc. on behalf of Poultry Science Association Inc. This is an open access article under the CC BY-NC-ND license (<http://creativecommons.org/licenses/by-nc-nd/4.0/>).

Received March 21, 2021.

Accepted November 4, 2021.

¹These authors contributed equally.

²Corresponding author: 472930822@qq.com

conditions, 26% of the fat in the liver comes from fatty acid de novo synthesis, and 15% from food (Sevastianova et al., 2012). The increased liver lipids induced by high carbohydrate foods is positively correlated with de novo fatty acid synthesis. The substrate of fatty acid de novo synthesis is mainly glucose, fructose, and amino acids (Basaranoglu et al., 2015). Ingested carbohydrates are the main stimulating factor for fatty acid de novo synthesis in the liver, and are more likely to induce fatty liver than fat in food. In non-alcoholic fatty liver disease, excessive carbohydrates are converted into fats and the increased fatty acid de novo synthesis is the main cause of liver lipid deposition (Ameer et al., 2014; Chung et al., 2014). High-sugar foods can activate liver fatty acid synthesis, and high-fat foods can inhibit this synthesis pathway. High-protein diet can reduce fat deposition induced by high-fat and high-sucrose diet in rats (Ferramosca et al., 2014). High-fructose foods increase fatty acid synthesis in the liver, leading to lipid deposition and IR in the liver (Montgomery et al., 2015). Large amounts of carbohydrates intake in the form of fructose and sucrose can induce fatty acid de novo synthesis. Fatty acid synthesis increase caused by high carbohydrate intake comes from the activation of transcription factors such as SREBP1, FAS, and ACC (Neuschwander-Tetri, 2013; Vos and Lavine, 2013). Excessive intake of sugar induces liver fat deposition and its influence on metabolism has been a hot research topic in recent years. However, the differences in liver lipid deposition induced by different types of sugars still lack systematic research.

The carbohydrate feed commonly used in livestock production, such as corn, wheat, and rice, is mainly composed of starch polysaccharide, which is digested in the body and absorbed by the small intestine as glucose and other simple sugars. A large number of animal studies have reported that high fructose diet can induce fatty liver (Todoric et al., 2020). When the geese or ducks were overfed with a high-energy diet which was rich in carbohydrates, their liver increased in size by 5 to 10 folds in 2 wk, which was accompanied by the occurrence of hepatic steatosis. The distinctive genetic characteristic of waterfowl was taken advantage of to produce *foie gras*. It had also been reported that high sucrose diet can induce lipid deposition by increasing the production of TG in vivo and decreasing the transport of TG (Eugenia D'Alessandro et al., 2014). Unlike human fatty liver disease, waterfowl is more likely to show nonpathological hepatic steatosis, and the functional integrity of the hepatocytes remains intact (Liu et al., 2016). Therefore, waterfowl is the model animals in biomedical research for overfed liver (Xu et al., 2018).

Foie gras, the fatty liver of overfed ducks or geese, is the most valued product resulting from waterfowl production systems. The fatty liver in geese, also called *foie gras*, is looked upon the delicious foods as caviar, black mushroom by the occidental, which has a rich, buttery, and delicate flavor. Consumers worldwide enjoy it, and there is a huge international market. This experiment explored the difference of lipid deposition regulatory

mechanism in goose liver from individual level, transcriptome level and cell level. Not only will understanding these differences between different types of sugar induced *foie gras* lipid deposition provide a method for improving *foie gras* quality, it is also conducive to improving the production efficiency. Meanwhile, it will provide not only a scientific basis to ensure animal welfare, but also an approach to the prevention and treatment of fatty liver disease in human.

MATERIALS AND METHODS

Ethics Statement

All procedures in the present study were subject to approval by the Institutional Animal Care and Use Committee (IACUC) of Sichuan Agricultural University (Permit No. DKY-B20141401), and carried out in accordance with the approved guidelines. All efforts were made to minimize the suffering of the animals. The movement of birds was not restricted before the age of 90 d. The experimental geese were killed with an electro-lethalizer before harvesting their liver samples.

Birds and Experiment Design and Sampling

One hundred and forty 13-wk-old male Tianfu Meat Geese came from Experimental Farm for Waterfowl Breeding at Sichuan Agricultural University (Ya'an, China), and the ganders were randomly separated into 5 groups (control group, corn overfeeding group, glucose overfeeding group, fructose overfeeding group, sucrose overfeeding group); the control group included 20 ganders, each overfeeding group was consisted of 30 ganders. The breed is a composite of 87.5% Landes (*A. anser*) and 12.5% of Sichuan White (*A. cygnoides*) and the population used in this study is closed and has been under selection for over 10 generations. The overfeeding procedure and diet regimes were performed as previously described (Wei et al., 2020), all the experimental geese were reared in cages with a density of 3 birds /m², the temperature was controlled at about 25°, and light was provided at night (dim light). The grouping situation and overfeeding dietary component was shown in Table 1. The ganders of control group were fed maize flour (dry matter: water = 1:1). In overfeeding group, the daily feed intake reached 1,600 g dry matters (4 meals a day; dry matter: water = 1:0.75), which lasted 3 wk. The falls and culling during the fattening period were shown in Supplementary material S-Figure 1 to S-Figure 5. All ganders were slaughtered when 16 wk old. After 12 h of fasting, the body weight of ganders was weighed before slaughter. Ten mL of blood were collected from wing vein, and then the ganders were killed. The serum was separated by blood centrifugation at 4°C for 4,000 r/min for 10 min, then kept at -20°C for follow-up detection. Six ganders of each group were anesthetized with intraperitoneal injection of sodium pentobarbital (60 mg/kg), and then killed; the liver was collected immediately. The livers were separated into 2

Table 1. Diet formula for experiment.

Items (%)	Control group (ad libitum)	corn flour Overfeeding group	Glucose Overfeeding group	Fructose Overfeeding group	Sucrose Overfeeding group
Feed intake (g / day)	300	1,600	1,600	1,600	1,600
Maize flour	100	94.5	85	85	85
Fish flour		2	2	2	2
NaCl		1	1	1	1
Soya oil		2.5	2	2	2
Glucose	-	-	10	-	-
Fructose	-	-	-	10	-
Sucrose	-	-	-	-	-
Total	100	100	100	100	100
Nutrient levels					
ME/ (MJ/kg)	12.87	14	14	14	14
Crude protein (CP)	8	8	8	8	8

parts respectively. A part of the liver tissue was frozen in liquid nitrogen immediately, and then kept at -80°C for transcriptome sequencing ($n = 3$) and long-chain fatty acid determination ($n = 6$). Other part of liver was washed in ice-cold saline (0.9% NaCl; 4°C) and fixed in 4% formaldehyde-phosphate buffer for histomorphology determination ($n = 3$). After slaughter, the liver was separated and weighed immediately ($n = 20$).

Cell Culture and Treatment

Hepatocytes were isolated from three 14-day-old Tianfu Meat Goose from the Experimental Farm for Waterfowl Breeding at Sichuan Agricultural University (Sichuan, China) using a modification of the "two-step procedure" described by Seglen (1976). Goose primary hepatocytes were isolated and cultured in dulbecco's modified eagle medium (DMEM) supplemented with 10% fetal bovine serum (PBS). The culture conditions were 37°C with 5% CO_2 after 24 h. And then, the cells were separately treated with serum-free media supplemented with 30 mmol/L glucose or fructose or sucrose and incubated for 24 h. Cell viability determination was shown in Supplementary material S-Figure 6. The cells were collected for follow-up study. Each experiment was performed at least in triplicate.

Concentration Measurement of Triglyceride and Very Low Density Lipoprotein

The extracellular very low density lipoprotein (VLDL) concentration in the supernatant was measured using a chicken VLDL ELISA kit (GBD, USA). The concentration of VLDL in the samples was determined by comparing the optical density (OD) value at 450 nm of the samples to the standard curve. After cultured cell treatment, the culture media was collected for detecting extracellular triglyceride (TG) concentration. Cell samples used to measure intracellular TG concentration were collected. The TG levels were quantified using a triglyceride GPO-POD assay kit (Biosinc, China). Measurements were in accordance with the manufacturer's protocol. All assays were performed in triplicate.

Oil Red O Staining

Briefly, after the treatments with goose primary hepatocytes, staining of intracellular lipids was performed using Oil Red O (Sigma, USA) according to the manufacturer instructions. Oil Red O staining images were taken using a light microscope (Olympus Optical, Tokyo, Japan) at $200\times$ magnification. For quantification of lipid accumulation, the Oil Red O-positive cells were extracted using 100% isopropanol for 10 min. The absorbance of the extracted dye was analyzed at a wavelength of 510 nm (BIO-RAD).

Measurement of Protein Content in Culture Cells

Protein content of fatty acid synthetase (FAS), acetyl-CoA carboxylase (ACC α), carnitine palmitoyltransferase 1 (CPT1), microsomal triglyceride transfer protein (MTP), and apolipoprotein B (APOB) in culture cells was measured using ELISA kit (GBD). Further measurements were in accordance with the manufacturer's protocol. All assays were performed in triplicate.

Isolation of Total RNA and RT-PCR

Cultured cells total RNA was extracted using extraction kit (TRIzol Reagent; Invitrogen, Thermo Fisher Scientific, China), and then RNA was transcribed into cDNA via reverse-transcription using the Primer Script TM RT system kit for real-time PCR (TaKaRa, Japan) as described by the manufacturer. The fluorescence quantitative PCR was performed on the CFX 96 instrument (Bio-Rad), using a Takara ExTaq RT-PCR kit and SYBR Green as the detection dye (Takara, Japan); qRT-PCR reaction system contained the newly generated cDNA template (1.0 μL), SYBR Premix Ex Taq TM (6.0 μL), sterile water (4.0 μL), upstream primers of target genes (0.5 μL) and downstream primers of target genes (0.5 μL). After initial denaturation at 95°C for 5 min, 40 cycles were carried out: 95°C for 10 s, 60°C for 20 s, 72°C for 15 s and 72°C extension for 10 min. Fluorescence quantitative PCR Primers (Beijing Genomics

institution, Beijing, China) designed according to the goose gene sequences in current experiment were summarized in Supplementary S-Table 1. Fold change in the expression of target gene was analyzed using the $2^{-\Delta\Delta C_t}$ method (Livak and Schmittgen, 2001). β -actin and 18S used as the internal reference gene. Each test includes 3 biological samples and each sample was analyzed in triplicate.

Protein Analysis by Western Blotting

Following the incubation with the different treatments, SDS buffer was used to extract total proteins from the harvested cells which were washed twice and collected in ice-cold PBS. The untreated cells were used as control. Equal amounts of total proteins (100 μ g/lane) were separated by sodium dodecyl sulfate polyacrylamide gel electrophoresis (SDS-PAGE) (6%) and transferred to a Polyvinylidene Fluoride (PVDF) membrane. After blocking with a mixture of 5% skimmed milk/Tris-buffered saline Tween 20 (TBST), the membranes were incubated overnight at 4°C with the primary antibody rabbit against sterol regulatory element-binding proteins-1 (SREBP1) (bs-1402R), carnitine palmitoyltransferase (CPT1A) (bs-2047R), microsomal triglyceride transfer protein (MTP) (bs-5083R) antibodies (1:1,000; Beijing Biosynthesis Biotechnology, China); antibody information was listed in Supplement materials S-Table2. Following three consecutive washes in TBST (0.05%), the membranes were incubated with the goat anti-rabbit horseradish peroxidase-conjugated IgG at 1:2,000 (Beijing Biosynthesis Biotechnology) for another 2 h at room temperature. The results were normalized to α -Tubulin (bs-0519R) (Beijing Biosynthesis Biotechnology) protein levels. Protein expression levels were finally visualized using enhanced chemiluminescence (ECL) reagents (Beyotime Institute of Biotechnology, China).

Biochemical Index Examinations of Serum

Ten individuals blood samples were selected randomly from each group, serum biochemical indices were quantified in whole serum. The assay kits that detected total protein (TP), total cholesterol (T-CHO), albumin (ALB), very low-density lipoprotein (VLDL), very high-density lipoprotein (VHDL), TG, blood glucose, insulin, alanine aminotransferase (ALT), aspartate aminotransferase (AST), uric acid (UA) were provided by Nanjing Jiancheng Bioengineering Institute (Nanjing, China);

Histomorphology Examinations

According to the methods of previous study (Cao et al., 2015), the cross-sections from the middle of liver were preserved in 4% formaldehyde-phosphate buffer were prepared using standard paraffin embedding techniques, sectioned (5 μ m) and stained with

hematoxylin and eosin (HE), and sealed by neutral resin size thereafter, and then examined by microscope photography system (Olympus, Tokyo, Japan), each slice was observed and 5 visual fields were randomly selected at 40 \times magnifications.

Long-Chain Fatty Acid of Foie Gras Determination

According to the methods described as previous experiment (Su et al., 2020). After grinding, 0.5 g liver sample was used to mix with 0.5 mL 0.5 g/l internal standard undecylenic acid methyl ester (Sigma), 2 mL 95% ethanol, 2 mL pure water and 0.1 g pyrogallol acid in a 50-mL screw-thread erlenmeyer flask, and then 10 mL HCL (8.3 mol/l) were added using water bath heating hydrolyzed the liver sample (80°C, 40 min). After hydrolysis, removed the flask and cooled it to room temperature. Hydrolysate was transferred to the separating funnel, and mixed with 50 mL diethyl ether/petroleum ether (1:1, v/v). After covered the lid, shook it for 5 min, and then let it stand for 10 min. Liquid supernatant was transferred to 500 mL flat-bottomed flask. Lipid extraction was repeated 3 times. After concentrated and dried the liquid supernatant via rotary evaporator under 55°C (the residue was lipid extracts), the flat-bottomed flask which contained the lipid extracts was linked condenser pipe and heated in 80°C water bath, and the lipid saponification (2% NaOH-Methanol, 30 min) was performed. And then the fatty acids methyl esterification (15% BF₃, 30 min) was performed. When the fatty acids methyl esterification finished, removed the flask from the water bath and cooled it down quickly to room temperature. Added 10 mL n-heptane into flask accurately, shook it 2 min, and added saturated sodium chloride solution, and stilled it. Removed the upper n-heptane extraction 5 mL to 15 mL tube, and 3 to 5 g anhydrous sodium sulfate was added, and shook it 1 min, stilled it for 5 min. And then, removed the upper solution into the sample bottle for determination.

Gas chromatography (GC; 7890, Agilent Technologies, USA) was used to detected the foie gras fatty acids. Fatty acid methyl esters were analyzed using a gas chromatograph fitted with a 0.25- μ m-thick film of reticulated polyethyleneglycol phase and 30 m \times 0.25 mm i.d. capillary column (HP-FFAP) with nitrogen as the carrier gas. Chromatographic column temperature programmed: 160°C retained 1 min, up to 220°C in 5°C/min, then retained 8 min; carrier gas is nitrogen; total flow velocity: 70 mL/min. Fatty acid methyl ester qualitative mixture was provided by Sigma. The detection was performed by Qingdao Sci-tech Innovation Co., Ltd (Qingdao, Shandong, China).

Transcriptome Sequencing and Analysis

A total amount of 1- μ g RNA per sample was used as input material for library sample preparations. Sequencing libraries were generated using NEBNext UltraTM

RNA Library Prep Kit for Illumina NexSeq500 (NEB, Beijing, China) following manufacturer's recommendations and index codes were added to attribute sequences to each sample. The library fragments were purified with AMPure XP system (Beckman Coulter, Beverly, MA). PCR products were purified (AMPure XP system) and library quality was assessed on the Agilent Bioanalyzer 2100 system. The clustering of the index-coded samples was performed on a cBot Cluster Generation System using TruSeq PE Cluster Kit v4-cBot-HS (Illumina, USA). After cluster generation, the library preparations were sequenced on an Illumina platform and paired-end reads were generated. The sequencing was performed by Baimike biological Technology Co., LTD (Beijing, China).

Raw reads of fastq format were processed through in-house perl scripts. Clean reads were obtained by removing reads containing adapter, reads containing ploy-N and low quality reads from raw reads. Hisat2 tools soft were used to map with reference genome of geese (*A. cygnoides*) reference genome (assembly Ans_Cyg_PRJNA183603_v1.0, https://www.ncbi.nlm.nih.gov/genome/31397?genome_assembly_id=229313). Differential expression analysis of 5 groups was performed using the DEseq. The resulting P values were adjusted using the Benjamini and Hochberg's approach for controlling the false discovery rate. Genes with an adjusted *P*-value < 0.05 found by DEseq were assigned as differentially expressed. We used KOBAS software to test the statistical enrichment of the differentially expressed genes (DEGs) in KEGG pathways. The sequences of the DEGs were blast to the genome of a related species (the protein protein interaction of which exists in the STRING database: <http://string-db.org/>) to get the predicted PPI of these DEGs. Transcriptome analysis was performed via Baimike biocloud platform (Baimike biological Technology Co., LTD, Beijing, China).

Statistical Analysis

By using SAS 9.13 package (SAS Institute Inc, Cary, NC), the comparisons of multiple groups were analyzed by GLM, and the means were assessed for significant differences using the SNK-q test. All data were presented as means \pm standard deviation (SD) and showed with graphs created with GraphPad Prism 5.0 software (GraphPad Prism Software, Inc.). We considered *P* < 0.05 as statistically significant.

RESULTS

The Effect of Glucose, Fructose, and Sucrose Treatment on the Lipid Deposition in Goose Primary Hepatocytes

Goose primary hepatocytes were treated with glucose, fructose, or sucrose 24 h. The lipid accumulation and gene and protein involved in lipid metabolism were detected. The relative mRNA expression of ACOX1,

CPT1A and PPAR γ were lower in sucrose treatment (*P* > 0.05; Figure 1B). The relative gene expression of MTP, ApoB, and DGAT2 were lower in sucrose treatment (*P* > 0.05; Figure 1C). The intracellular TG and T-CHO concentration was higher in sucrose and fructose group (*P* < 0.05; Figure 1D). As shown the intracellular lipid droplets observed from Oil red O staining (Supplementary material S-Figure 7), lipid deposition increased (*P* < 0.05), and the intracellular lipid content was higher in fructose and sucrose treatment (*P* < 0.05; Figure 1E).

Comparison of Different Type of Sugar on Slaughter Performance, Fatty Acid Composition, and Serum Parameters

As shown in Figure 2A, the body weights of overfed ganders were significantly higher than that of control geese (*P* < 0.05), but the 4 overfeeding were no difference (*P* > 0.05). The liver weight of fructose and sucrose overfeeding ganders was significantly higher than glucose overfeeding geese (*P* < 0.05). While the proportion of liver weight in sucrose overfeeding group was significantly increasing the most in relative weight by 3.44-fold than that in the control overfeeding group (*P* < 0.05). The ratio of liver weight to overfeed diet consumption is highest in sucrose overfeeding group. The mortality of sucrose overfeeding group was higher than that of fructose overfeeding group (26.66 vs. 13.33%) (Supplementary material S-Figure 1–S-Figure 5). As shown in Figure 2B, the size of the liver has increased significantly after overfeeding, HE staining of liver showed that the hepatocytes are homogeneous in size and the nucleus was clearly visible in the control group, which indicated that there is a serious TG accumulation in liver, especially in the fructose and sucrose overfeeding group. The size of goose fatty liver of fructose and sucrose overfeeding group is largest. Fatty acid composition of liver was measured as shown in Figure 3A, the content and proportion of unsaturated fatty acids significantly increased in overfeeding groups. At the same time, the content of n-3 polyunsaturated fatty acids (PUFA) and the ratio of n-3 PUFA to n-6 PUFA in the sugar-overfeeding group were significantly higher than those in the corn overfeeding group, which suggesting that supplementation with sugar can increase the n-3 polyunsaturated fatty acids content and ratio of n-3 PUFA to n-6PUFA in goose fatty liver formation (Figure 3B).

The results of the analysis of the effects of different sugars on the serum biochemical indexes of the overfed ganders are shown in Table 2. The TG level of the corn overfeeding group was significantly lower than that of the glucose, fructose, and sucrose overfeeding groups (*P* < 0.05). In the blood sugar level, the control group was significantly higher than the sugar treatment group (*P* < 0.05), indicating that overfeeding caused the impaired blood sugar function of the goose, however, the insulin level was not different significantly (*P* > 0.05). ALT concentration of fructose overfeeding group was significantly higher

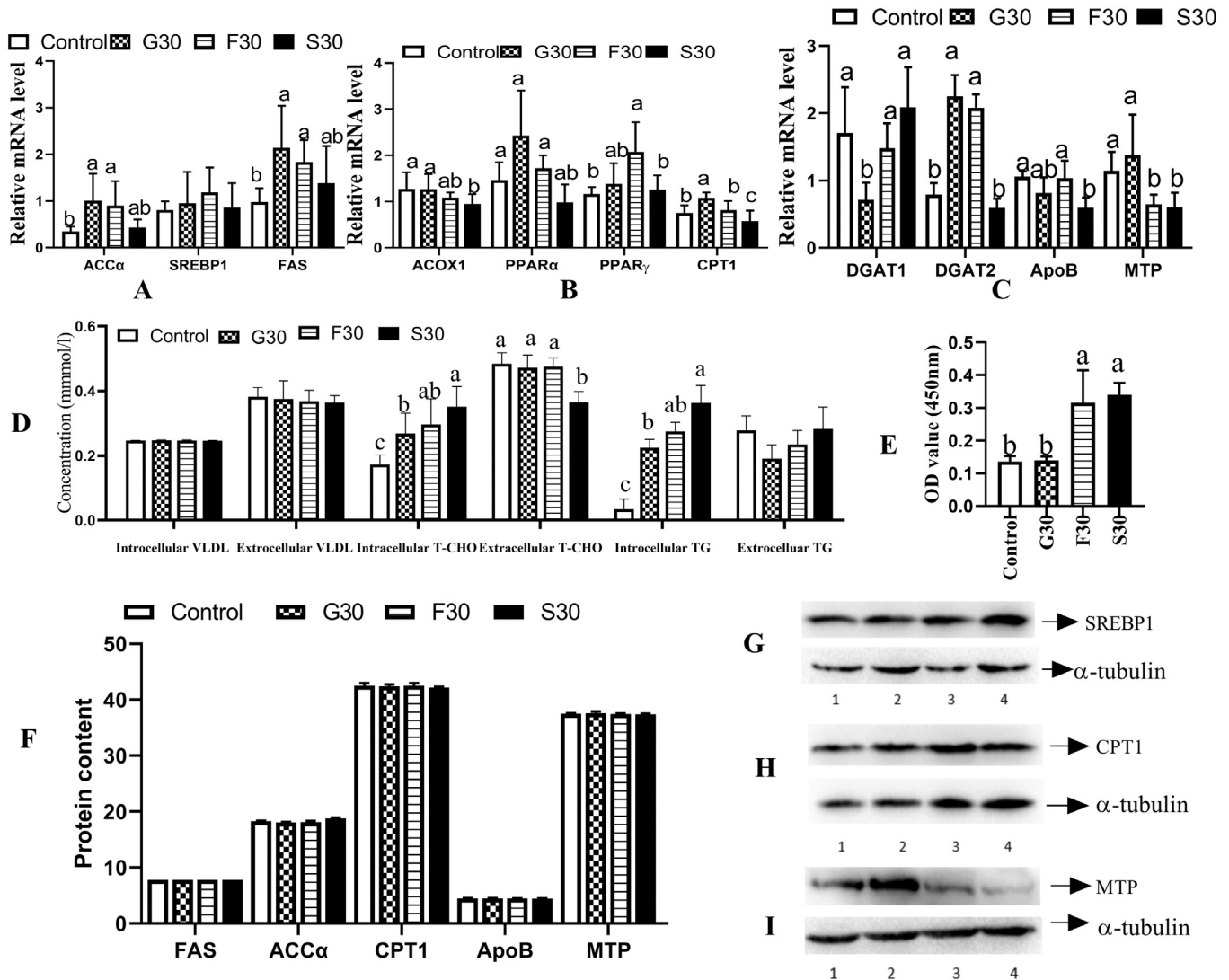


Figure 1. Effect of different types of sugar (glucose, fructose, and sucrose) on lipid metabolism in goose primary hepatocytes. (A) Relative mRNA level of ACC α , SREBP-1, and FAS, which is related to lipogenesis. (B) Relative mRNA level of ACOX1, PPAR α , PPAR γ , and CPT1, which is related to fatty acid oxidation. (C) Relative mRNA level of DGAT1, DGAT2, ApoB and MTP, which is related to lipids transportation. (D) Protein content of FAS, ACC α , ApoB and CPT1 (unit of FAS is nmol/mL; unit of ACC α is ng/mL; unit of CPT1 is ng/mL; unit of ApoB is nmol/mL). (E) Intracellular and extracellular VLDL concentrations. (F) Intracellular and extracellular T-CHO concentrations. (G) Intracellular and extracellular TG concentrations. (H) Intracellular lipid contents. Values are means \pm SD ($n = 3$). Different lowercase letters in the same set indicate difference among treatments at $P < 0.05$. G30, F30, and S30 represents the goose primary hepatocytes were treated with 30 mmol/L glucose, 30 mmol/L fructose and 30 mmol/L sucrose, respectively. The numbers “1, 2, 3, 4” under the blot indicates the treatment of control, 30 mmol/L glucose, 30 mmol/L fructose and 30 mmol/L sucrose, respectively. Abbreviations: ACC α , acetyl-CoA carboxylase; ACOX1, acyl-CoA oxidase 1; ApoB, apolipoprotein B; CPT1, carnitine palmitoyltransferase; DGAT1, diacylglycerol acyltransferase-1; DGAT2, diacylglycerol acyltransferase-2; FAS, fatty acid synthetase; MTP, microsomal triglyceride transfer protein; PPAR α , peroxisome proliferators-activated receptor- α ; PPAR γ , peroxisome proliferators-activated receptor- γ ; SREBP-1, sterol regulatory element-binding proteins-1; TG, triglyceride; VLDL, very low-density lipoprotein.

than that of control and sucrose overfeeding groups ($P < 0.05$).

Comparison Analysis on the Effect of Supplementation With Different Type of Sugar on Goose Fatty Liver Formation From Transcriptome Analysis

In this study, 12 cDNA libraries were constructed (Supplementary material S-Table 3 and S-Table 4), each RNA-seq library produced more than 107 million raw reads, 53 million clean reads and the clean data of

each sample reached 9.38GB. The quality scores (Q30) of all samples were above 94.28%. The percentage of total reads mapped to the *Anser* reference genome was between 72.79 and 74.99%, the percentages of reads uniquely mapped to the reference genome were all above 71.04%. These results demonstrated that the RNA-seq data was reliable and suitable for further analysis.

We identified DEGs by DEGseq software, and FDR and \log_2FC were used for screen the DEGs. The screening conditions were set at $FDR < 0.05$ and $|\log_2FC| > 1$. According to the distance calculated, the clustering diagram can directly demonstrate the distance and difference between samples. Cluster Analysis of the DEGs

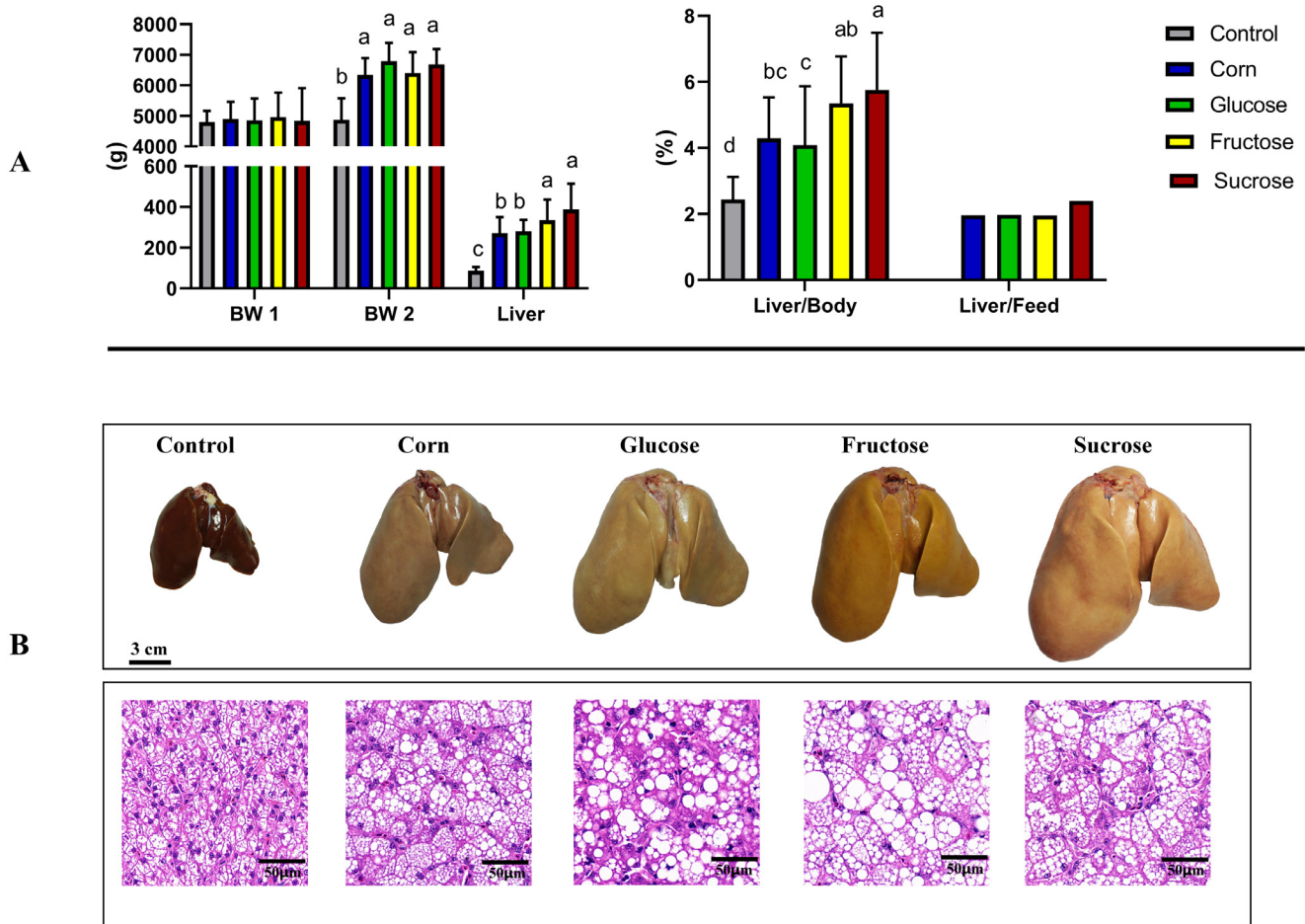


Figure 2. Effect of different types of sugar (glucose, fructose and sucrose) on *foie gras* performance in overfed goose. (A) Comparison of slaughter performance ($n = 20$). (B) Comparison of livers and liver tissue sections. (Liver tissue sections: [HE staining, $200\times$]; $n = 3$). Values are means \pm SD. Different lowercase letters in the same set indicate difference among treatments at $P < 0.05$. BW1, Body weight before overfeeding; BW2, Body weight after overfeeding; Liver/Body, The ratio of liver weight to body weight after overfeeding; Liver/Feed, The ratio of liver weight to overfeed diet consumption.

suggested that the Control group was the most different from the G, F, and S group, the G, F, and S group were aggregated in another branch (Figure 4A), but sample of G and F group were not in a separate branch, and the S group was separated from any groups, so we pay more attention to the DEGs of S group which were both specifically the consistency among biological replicates within groups, and to those are significantly different in fatty liver producing performance.

A total number of DEGs identified between C group and S group (Control-vs.-Sucrose) was 1,551, which were 827 upregulated and 724 downregulated genes shown in Supplementary material S-Table 5, Figures 4B and 4C. And the Control group with the Glucose group (Control-vs.-Glucose) was 1,535 DEGs in all, it contains 833 upregulated and 652 downregulated DEGs, while the Control group with the Fructose group (Control-vs.-Fructose) was 1,659 DEGs in all, and contains 959 upregulated and 700 downregulated DEGs.

In order to gain a further understanding of goose fatty liver formation difference induced by glucose, fructose and sucrose, the KEGG database was used for annotate and analyze the DEGs pathways. As shown in Figure 5 and Supplementary material S-Figure 8, the highest enrichment signal pathways related to DEGs in

the corn overfeeding group are: fatty acid metabolism, unsaturated fatty acid synthesis (biosynthesis of unsaturated fatty acids), peroxisome, steroid biosynthesis, and fatty acid elongation (Figure 5A). The highest enrichment of DEGs-related signaling pathways in the glucose overfeeding group was: Cell cycle, fatty acid extension, DNA replication, and PPAR signaling pathway (Figure 5B). The highest enrichment DEGs-related signaling pathways of the fructose overfeeding group are: peroxisomes, fatty acid metabolism, unsaturated fatty acid synthesis pathway, PPAR signaling pathway, and adipocytokine signaling pathway, sterol biosynthesis, fatty acid extension (Figure 5C). The highest enrichment of DEGs-related signaling pathways in the sucrose overfeeding group were: fatty acid extension, fatty acid metabolism, unsaturated fatty acid synthesis, PPAR signaling pathway, and adipocyte factor signaling pathway (Figure 5D).

DISCUSSION

When the content of TG produced far exceeded the transport capacity of apolipoproteins, and the fatty acid produced far exceeded the degraded fatty acid by

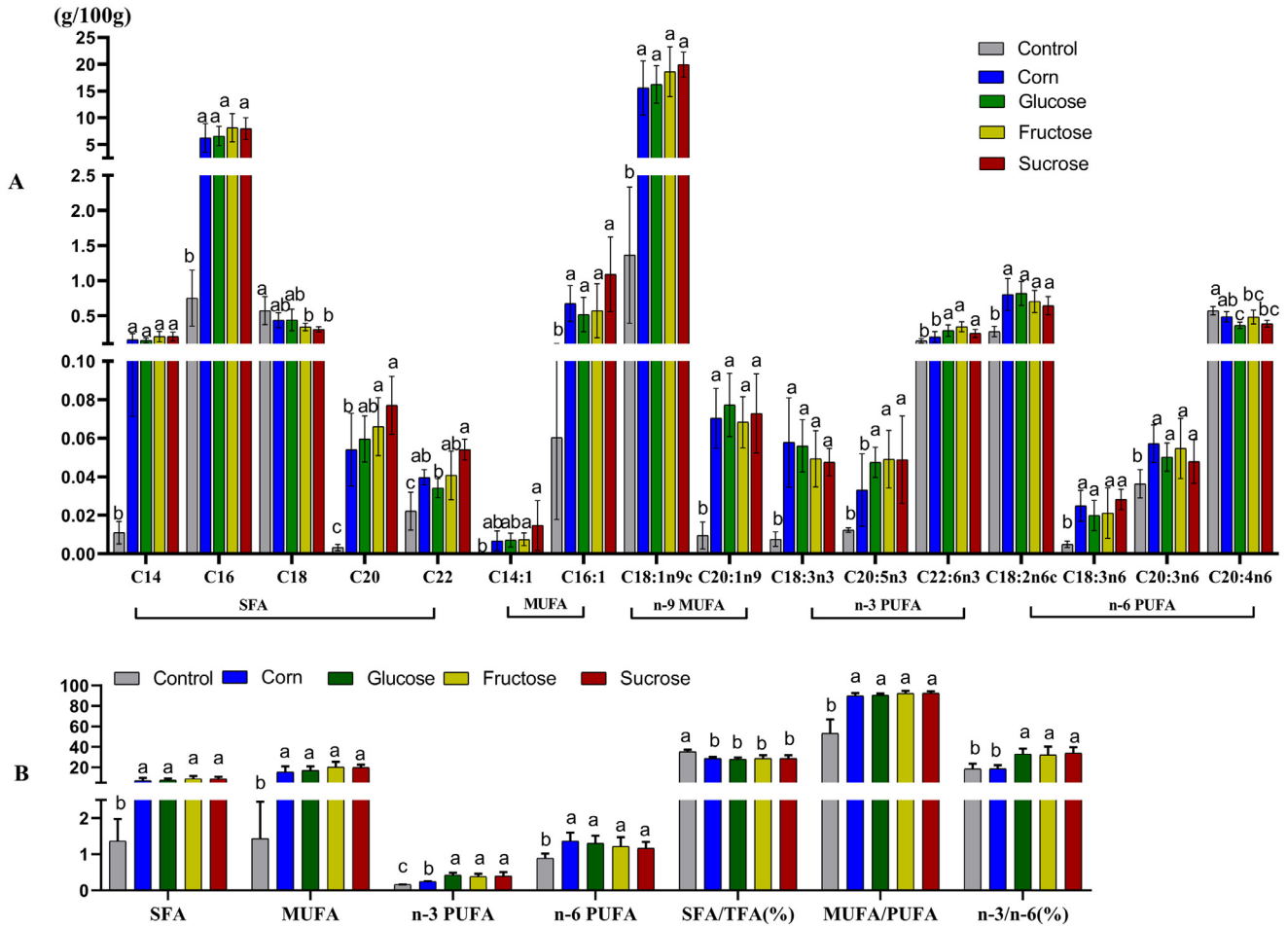


Figure 3. Effect of different types of sugar (glucose, fructose, and sucrose) on fatty acid composition (n = 6). (A) Comparison of fatty acid composition. (B) Statistical result of fatty acid content (unit of SFA, MUFA, and PUFA is “g/100 g”). Values are means \pm SD. Different lowercase letters in the same set indicate difference among treatments at $P < 0.05$. Abbreviations: MUFA, monounsaturated fatty acid; PUFA, poly-unsaturated fatty acid; SFA, saturated fatty acid.

β -oxidation, the accumulation of lipids occurred (Wei et al., 2021), which is the mechanism of fatty liver formation. The results of this experiment showed that after the primary goose hepatocytes were treated with glucose, fructose and sucrose, the content of intracellular TG increased, and the oil red O test results also showed that glucose, fructose and sucrose treatments can induce lipid deposition in goose primary hepatocytes. When the

goose primary hepatocytes were treated with glucose, fructose and sucrose, respectively, the expression levels of FAS, ACC α and other genes related to fatty acid synthesis significantly increase. We also found that there was a tendency to decrease the expression levels of key genes involved in the fatty acid transportation, which indicated that fructose and sucrose treatment reduced fatty acid oxidation (Figure 1). It suggested that

Table 2. The effects of different sugars on serum biochemical indexes in overfed geese.

Items	Control group	Corn overfeeding group	Glucose overfeeding group	Fructose overfeeding group	Sucrose overfeeding group
TG (mmol/L)	2.69 \pm 0.53 ^c	4.07 \pm 0.82 ^b	5.66 \pm 1.66 ^a	5.48 \pm 0.46 ^a	5.84 \pm 1.13 ^a
T-CHO (mmol/L)	11.94 \pm 3.97 ^b	27.28 \pm 6.18 ^a	31 \pm 8.38 ^a	33.58 \pm 8.61 ^a	31.74 \pm 5.96 ^a
VHDL (mmol/L)	8.42 \pm 1.57 ^b	15.4 \pm 2.25 ^a	15.68 \pm 4.84 ^a	17.2 \pm 6.43 ^a	17.82 \pm 4.32 ^a
VLDL (mmol/L)	1.53 \pm 0.66 ^b	2.72 \pm 1.15 ^{ab}	4.39 \pm 2.49 ^a	5.12 \pm 2.94 ^a	5.01 \pm 1.3 ^a
Glucose (mmol/L)	8.43 \pm 1.08 ^a	5.25 \pm 0.96 ^c	6.51 \pm 1.22 ^{bc}	6.39 \pm 0.93 ^{bc}	7.05 \pm 0.82 ^b
Insulin (μ IU/L)	72.49 \pm 19.85	62.18 \pm 18.81	55.69 \pm 14.98	68.92 \pm 24.22	68.47 \pm 12.57
ALT (U/gprot)	37.87 \pm 22.81 ^b	44.95 \pm 22.03 ^{ab}	41.89 \pm 20.53 ^{ab}	70.79 \pm 27.39 ^a	35.71 \pm 7.78 ^b
AST (U/gprot)	61.27 \pm 15.65	45.9 \pm 13.41	44.43 \pm 29.07	69.56 \pm 23.47	52.88 \pm 22.04
TP (μ g/ML)	2,329.02 \pm 155.03 ^b	2,216.56 \pm 163.84 ^b	3,142.46 \pm 79.27 ^a	3,095.03 \pm 118.44 ^a	2,947.62 \pm 230.25 ^a
ALB (μ g/ML)	20.57 \pm 3.79 ^b	22.22 \pm 5.86 ^b	21.67 \pm 6.64 ^b	24.86 \pm 3.57 ^{ab}	29.21 \pm 5.37 ^a
UA (μ mol/L)	235.97 \pm 68.19 ^b	465.93 \pm 171.07 ^{ab}	668.18 \pm 281.09 ^a	678.67 \pm 375.96 ^a	570.8 \pm 114.43 ^a

Abbreviations: ALT, alanine aminotransferase; AST, aspartate aminotransferase; TG, triglyceride; T-CHO, total cholesterol; TP, total protein; ALB, albumin; VHDL, very high-density lipoprotein; VLDL, very low-density lipoprotein, insulin; UA, uric acid.

The data in the table is expressed as mean \pm SD (n = 10); the same letter (ab) between each line of data indicates that the difference is not significant ($P > 0.05$), the letter between each line of data is different, indicating that the difference is not significant ($P < 0.05$).

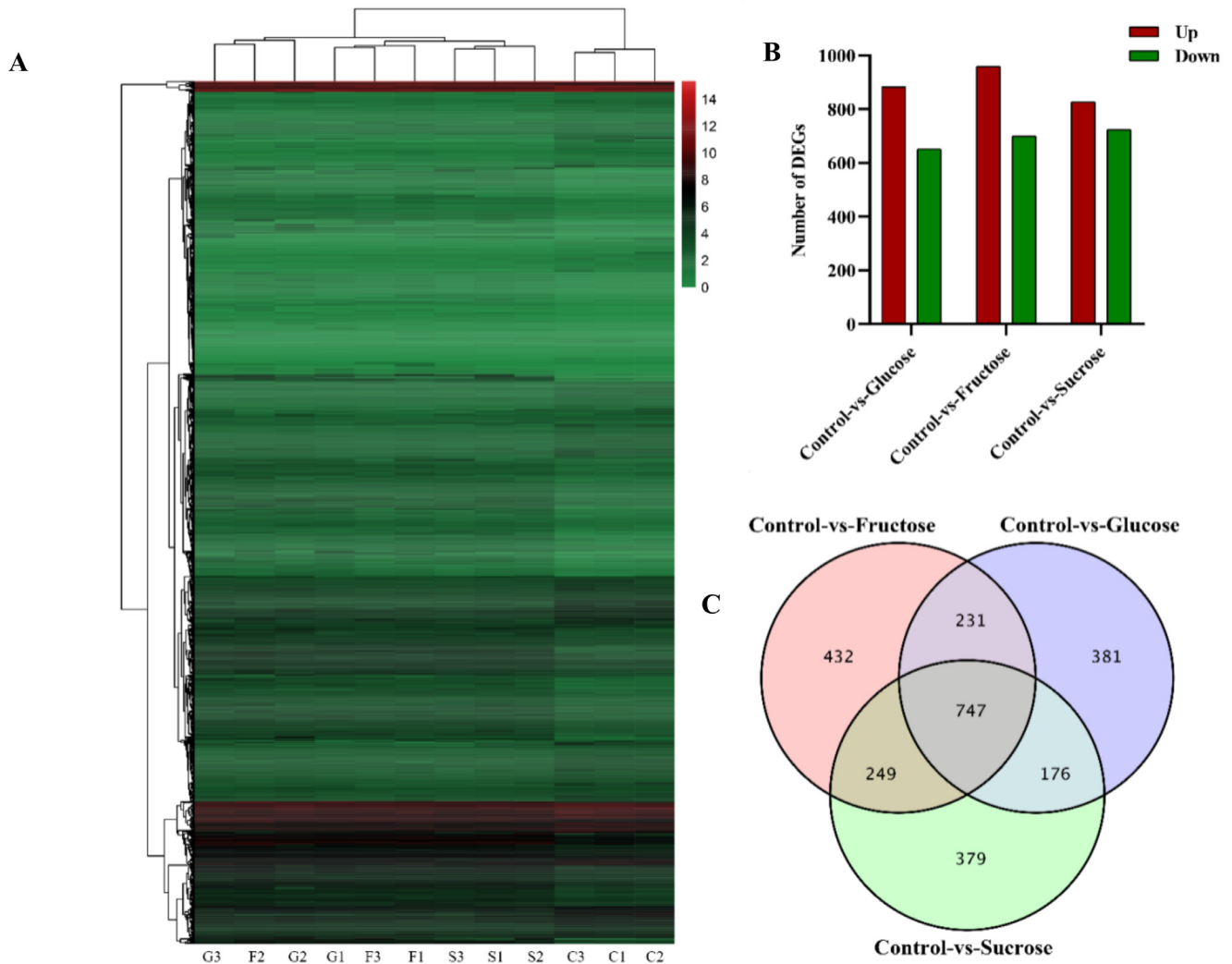


Figure 4. mRNA transcriptome analysis of differentially expressed genes (DEGs) in goose fatty liver induced by different types of sugar (glucose, fructose, and sucrose) ($n = 3$). (A) Heatmap analysis of DEGs. $P < 0.05$, \log_2 (fold change) > 1 . (B) Number of DEGs. (C) Venn diagram of the DEGs. C1-C3: control group; G1-G3: glucose overfeeding group; F1-F3: fructose overfeeding group; S1-S3: sucrose overfeeding group.

fructose and sucrose can decrease lipids transportation. Thereby, the fructose and sucrose treatment increased the lipids deposition in goose primary hepatocytes.

Goose fatty liver (*foie gras*) has a special hepatic steatosis process where lipid deposition accompanies with cell proliferation (Wei et al., 2020a). KEGG enrichment pathways showed that the DEGs in overfeeding group were mainly enriched in fatty acid metabolism, unsaturated fatty acid synthesis, PPAR signaling pathway and cell cycle pathway. In overfeeding process, due to the intake of carbohydrates increase, significant changes have taken place in the signaling pathways related to metabolism, especially the signaling pathways related to lipid metabolism. Transcriptome analysis showed that in corn overfeeding group, fatty acid metabolism and lipid deposition induced by sterol synthesis are the major way in the formation of goose fatty liver. Different from corn overfeeding, the PPAR signaling pathway is highly enriched in the fructose and sucrose overfeeding groups. The PPAR pathway regulates lipid metabolism, participates in fat cell differentiation (Wang et al., 2014; Liu et al., 2020). The liver-type fatty acid binding

protein (**FABP1**) can specifically bind to fatty acids and has a transport effect on fatty acids. It is an important fatty acid carrier protein in the cell. It not only participates in the absorption, transport and metabolism of fatty acids, but also has antioxidant effects and regulates cell growth and proliferation (Xu et al., 2019; Ho et al., 2020). In this study, FABP1 gene expression in the sucrose overfeeding group was significantly lower than that in glucose and fructose overfeeding groups (Supplementary material S-Figure 8A), which indicated that the liver lipid transport function of the sucrose overfeeding group was lower than that of glucose and fructose, so more lipids deposited in the goose liver. In the glucose overfeeding group, cell cycle and DNA replication pathways were highly enriched, suggesting that more cell proliferation occurred in the goose liver of glucose overfeeding group. The regeneration process of the hepatocytes is extremely complex and regulated by many factors. Cyclin Dependent Kinase (**CDKs**) is the core of the entire cell cycle regulatory protein. CDKs can only be activated to perform their functions after combining with the corresponding cell cycle regulatory

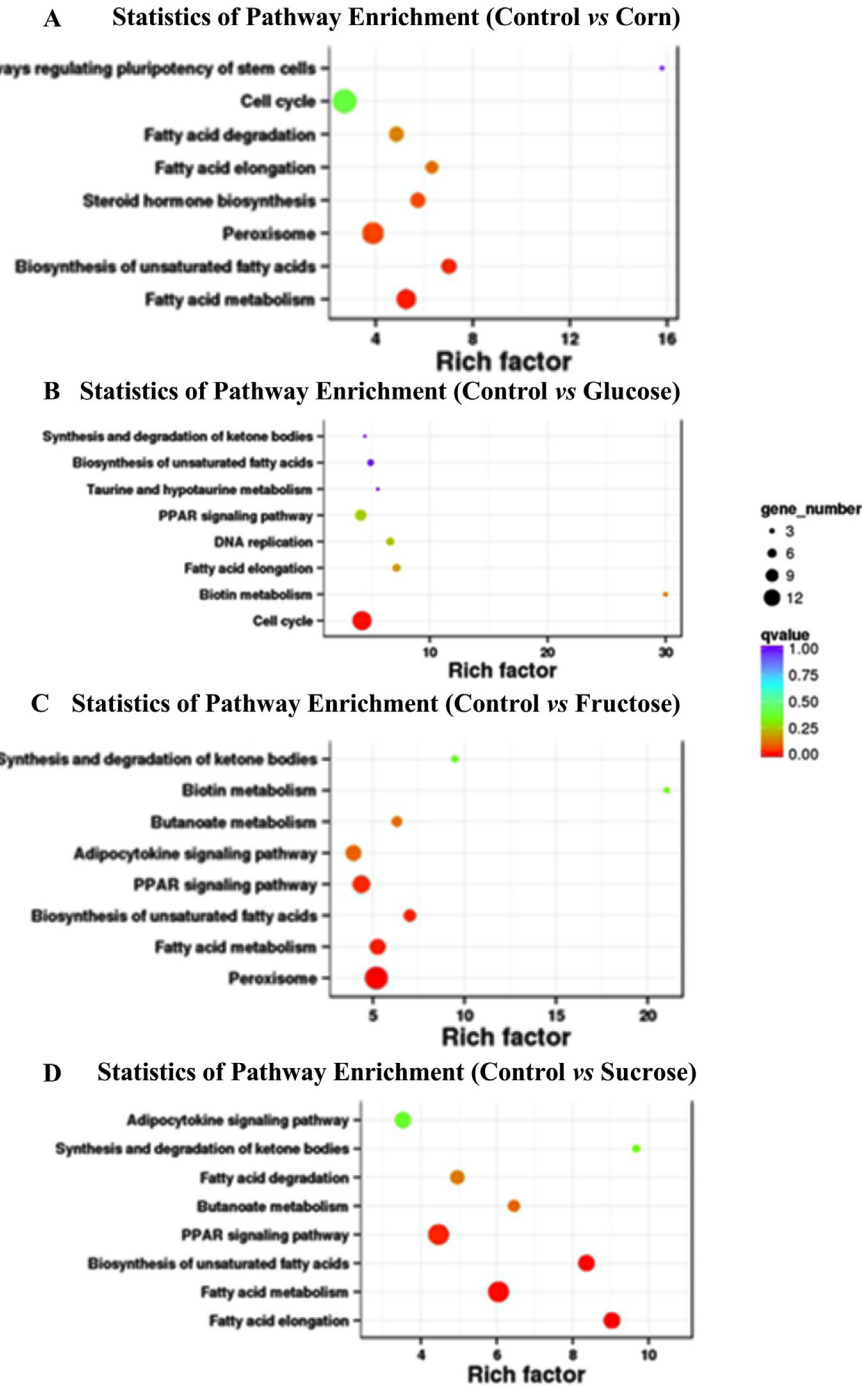


Figure 5. Gene ontology classifications and KEGG enrichment pathways ($n = 3$). (A) Control group vs. corn overfeeding group. (B) Control group vs. glucose overfeeding group. (C) Control group vs. fructose overfeeding group. (D) Control group vs. sucrose overfeeding group. The ordinate represents the path name and the abscissa is the enrichment factor. The higher the enrichment factor, the more significant the enrichment level of differentially expressed genes in this pathway. The color of the circle represents q-value, and the smaller q-value is, the more reliable the enrichment significance of differentially expressed genes in this pathway is. The size of the circle indicates the number of genes enriched in the pathway. The larger the circle, the more genes there are.

protein to form a CDKs-cyclin complex (Campbell et al., 2020). In this experiment, the gene expression of *CDK1* was significantly increased in the overfeeding group, especially the glucose overfeeding group, indicating that glucose promoted the mitosis of hepatocytes and induced the proliferation and meristem of hepatocytes. *CDC7*, *CCNA2*, *CCNB2*, *ATR*, and *BUB1B* are also genes related to cell cycle progression (Winston, 2001; Rao et al., 2009; Pereira et al., 2020). In this experiment,

the expression levels of *CDK1*, *CDC7*, *CCNA2*, *BUB1B* in the glucose overfeeding group were the highest (Supplementary material S-Figure 8). Our other studies also showed that glucose can regulate cell growth and proliferation through cell cycle and apoptosis pathways (Han et al., 2016; Wei et al., 2017).

Insulin is the only hormone in the body that can lower blood sugar. Insulin resistance (IR) refers to the decreased sensitivity of the insulin target organs (mainly

liver, skeletal muscle, and adipose tissue), that is, the biological effect of normal dose of insulin is lower than the normal one. The IR caused by different types of carbohydrate metabolism is different. Long-term high-dose fructose and sucrose intake can trigger the stress response in hepatocytes and impair insulin signals, which induced IR. Fructose may also reduce insulin sensitivity by changing the intestinal microflora or changing intestinal permeability, long-term high-dose fructose diet leads to glucose and lipid metabolism disorders, and ultimately leads to the IR (Cani et al., 2007), which in turn can aggravate the symptoms of metabolic syndrome. Fructose intake is closely related to the IR increase (Cecilia et al., 2015; Lin et al., 2016). In mammals, IR plays a role in the development of non-alcoholic fatty liver disease. Fatty liver caused by high fructose intake may be related to IR (Song et al., 2012). As demonstrated by Geng et al. (2015), overfeeding causes IR. Sucrose is a disaccharide which is made up of 50% fructose and 50% glucose. Studies believe that fructose component is the reason why sucrose metabolism decreased liver insulin sensitivity (Wei et al., 2007). In this experiment, the liver weight of fructose and sucrose overfeeding group were higher, one of reason may be IR induced by fructose intake. In addition, more and more studies believe that high fructose intake is the main cause of non-alcoholic fatty liver (Neuschwander-Tetri, 2013; Vos and Lavine, 2013). Some studies believe that high-dose fructose and sucrose foods can significantly increase liver fat content. Fructose has a more pronounced effect than sucrose, and a monosaccharide has a more obvious effect than polysaccharide (Siddiqui et al., 2015), which is consistent with the results of other studies (Pickens et al., 2010; Roncal-Jimenez et al., 2011).

Blood parameters are regarded as the one of indicators of whether disease happens or not. In respect of liver inflammation assessment, traditional liver enzymes, such as AST and ALT have been applied clinically to assess hepatocyte damage and exclude NASH (Undamatla et al., 2020; Zhou et al., 2020). The elevation of blood TG, TC, HDL, ALB, ALT, and AST is frequently associated with fatty livers in mammalian animals. In this experiment, the ALT level of the fructose overfeeding group was significantly higher than that of the sucrose overfeeding group and the corn overfeeding group; in addition, the TP and ALB as the indices reflecting the function of the liver protein synthesis and storage (Durgappa et al., 2019), the decrease of their contents indicated that the ability of liver to synthesize protein was weakened (Wang et al., 2015), the ALB levels of the corn overfeeding group and the glucose overfeeding group were significantly lower than the sucrose overfeeding group. It suggested that although the chronic hepatitis occurred in sucrose overfeeding group, the hepatocyte was not seriously injured and the liver function was not affected, which showed that the inflammation inhibition mechanism existed in goose liver (Geng et al., 2016a). It has been reported that the unsaturated fatty acids (UFA) could inhibit SFA-induced elevation of ceramides and inflammation

(Schwartz et al., 2010). The fatty liver of goose is more common in UFA when compared to the mammalian fatty liver, with the polyunsaturated fatty acids in particular, such as omega-3 and omega-6 (Tang et al., 2018), that is, the content of SFA is 39 to 47% in the fatty liver of overfed goose (Allard et al., 2008); the content of SFA is 52 to 56% in the liver of human suffered from NAFLD (Molette et al., 2001). It has also been reported that multiple fatty acid desaturase including stearoyl-CoA desaturase were induced in the liver of the overfed geese (Geng et al., 2016b). In this experiment, the liver of the sucrose overfeeding group contained a lot of unsaturated fatty acids, especially (n-3) polyunsaturated fatty acids. It may be one of the reasons that the sucrose overfeeding group had higher liver weight than the corn, glucose and fructose overfeeding group.

CONCLUSIONS

Glucose, fructose, and sucrose can all induce the lipid deposition in overfed goose liver, however, the regulatory mechanism is different. The PPAR signaling pathway is highly enriched in the lipid deposition process induced by fructose and sucrose, glucose enriched cell cycle and DNA replication pathways in goose fatty liver formation. In addition, sucrose and fructose have better inducement of lipid accumulation in goose fatty liver formation. This experiment is only a preliminary exploration on the regulatory mechanism of lipid deposition by different type of sugar in goose liver, further mechanistic differences are needed further study. For example, the relationship between lipid deposition, insulin resistance and endoplasmic reticulum stress in the hepatocytic steatosis induced by different sugar type has been not clearly elucidated. Study result indicated that overfeeding dietary 10% fructose or 10% sucrose supplementation induce more lipid deposition in *foie gras*, however, whether overfeeding dietary supplementation with high concentration of fructose or sucrose in can reduce overfeeding intensity or shorten the overfeeding time need to be further research.

In *foie gras* production, the most common feed is maize flour and maize pellet. In current overfeeding experiment, the main ingredient of overfeeding feed is maize flour. Compared with maize pellet in overfeeding, the advantages of maize flour are high fluidity, fast overfeeding speed and lower mortality, etc., however, the advantages are overfeeding times increase and *foie gras* weight is lighter; therefore, maize pellet are still used in *foie gras* production mostly. Although the weight of *foie gras* produced via maize pellet overfeeding is higher, the overfeeding speed is slower and the mortality is higher than corn flour. So, how to overcome the shortcomings of overfeeding using corn flour becomes a problem that is necessary to be solved. In this current study, we found that fructose and sucrose have good induction for lipid deposition in goose liver, which can be a reference to improve maize flour overfeeding effect.

ACKNOWLEDGMENTS

The work was supported by the National Natural Science Funds of China (No. 31672413), and the National Waterfowl Industrial Technology System (No. CARS-43-6).

Availability of data and materials: The supplement materials and original source data of this paper were uploaded to Figshare, the Publically available DOI for Figshare: <https://figshare.com/s/70fbe6ff915e6471c431>; Transcriptome analysis was performed via Baimike biocloud platform (<https://international.biocloud.net/zh/dashboard>; ID:15215045770; Password: deng19940227).

DISCLOSURES

No conflict of interest exists in the submission of this manuscript, and manuscript is approved by all authors for publication.

SUPPLEMENTARY MATERIALS

Supplementary material associated with this article can be found in the online version at [doi:10.1016/j.psj.2022.101729](https://doi.org/10.1016/j.psj.2022.101729).

REFERENCES

Allard, J. P., E. Aghdassi, S. Mohammed, M. Raman, G. Avand, B. M. Arendt, P. Jalali, T. Kandasamy, N. Prayitno, M. Sherman, M. Guindi, D. W. L. Ma, and J. E. Heathcote. 2008. Nutritional assessment and hepatic fatty acid composition in non-alcoholic fatty liver disease (NAFLD): a cross-sectional study. *J. Hepatol.* 48:300–307.

Ameer, F., L. Scandiuzzi, S. Hasnain, H. Kalbacher, and N. Zaidi. 2014. De nova lipogenesis in health and disease. *Metab. Clin. Exp.* 63:895–902.

Basaranoglu, M., G. Basaranoglu, and E. Bugianesi. 2015. Carbohydrate intake and nonalcoholic fatty liver disease: fructose as a weapon of mass destruction. *Hepatobiliary Surg. Nutr.* 4:109–116.

Campbell, G. J., E. L. Hands, and M. Van de Pette. 2020. The role of CDKs and CDKIs in murine development. *Int. J. Mol. Sci.* 21:5343, doi:10.3390/ijms21155343.

Cani, P. D., J. Amar, M. A. Iglesias, M. Poggi, C. Knauf, D. Bastelica, A. M. Neyrinck, F. Fava, K. M. Tuohy, C. Chabo, A. Waget, E. Delmee, B. Cousin, T. Sulpice, B. Chamontin, J. Ferrieres, J.-F. Tanti, G. R. Gibson, L. Casteilla, N. M. Delzenne, M. C. Alessi, and R. Burcelin. 2007. Metabolic endotoxemia initiates obesity and insulin resistance. *Diabetes.* 56:1761–1772.

Cao, W., G. Liu, T. Fang, X. Wu, G. Jia, H. Zhao, X. Chen, C. Wu, J. Wang, and J. Cai. 2015. Effects of spermine on the morphology, digestive enzyme activities, and antioxidant status of jejunum in suckling rats. *RSC Adv.* 5:76607–76614.

Cecilia, C., M., M. L. Massa, L. Gonzalez Arbelaez, G. Schinella, J. J. Gagliardino, and F. Francini. 2015. Fructose-induced inflammation, insulin resistance and oxidative stress: a liver pathological triad effectively disrupted by lipoic acid. *Life Sci.* 137:1–6.

Chung, M., J. Ma, K. Patel, S. Berger, J. Lau, and A. H. Lichtenstein. 2014. Fructose, high-fructose corn syrup, sucrose, and nonalcoholic fatty liver disease or indexes of liver health: a systematic review and meta-analysis. *Am. J. Clin. Nutr.* 100:833–849.

Durgappa, M., V. Saraswat, G. Pande, S. Mohindra, A. S. Bhadauria, and S. P. Butala. 2019. Slow continuous infusion of diuretic, albumin and/or terlipressin in patients with severe alcoholic hepatitis and acute on chronic liver failure. *J. Gastroenterol. Hepatol.* 34:424.

Eugenia D'Alessandro, M., M. Eugenia Oliva, M. Alejandra Fortino, and A. Chicco. 2014. Maternal sucrose-rich diet and fetal programming: changes in hepatic lipogenic and oxidative enzymes and glucose homeostasis in adult offspring. *Food Funct.* 5:446–453.

Ferramosca, A., A. Conte, F. Damiano, L. Siculella, and V. Zara. 2014. Differential effects of high-carbohydrate and high-fat diets on hepatic lipogenesis in rats. *Eur. J. Nutr.* 53:1103–1114.

Geng, T., L. Xia, F. Li, J. Xia, Y. Zhang, Q. Wang, B. Yang, S. Montgomery, H. Cui, and D. Gong. 2015. The role of endoplasmic reticulum stress and insulin resistance in the occurrence of goose fatty liver. *Biochem. Biophys. Res. Commun.* 465:83–87.

Geng, T. Y., B. Yang, F. Y. Li, L. L. Xia, Q. Q. Wang, X. Zhao, and D. Q. Gong. 2016a. Identification of protective components that prevent the exacerbation of goose fatty liver: characterization, expression and regulation of adiponectin receptors. *Comp. Biochem. Physiol. B-Biochem. Mol. Biol.* 194:32–38.

Geng, T. Y., X. Zhao, L. L. Xia, L. Liu, F. Y. Li, B. Yang, Q. Q. Wang, S. Montgomery, H. M. Cui, and D. Q. Gong. 2016b. Supplementing dietary sugar promotes endoplasmic reticulum stress-independent insulin resistance and fatty liver in goose. *Biochem. Biophys. Res. Commun.* 476:665–669.

Han, C., S. Wei, Q. Song, F. He, X. Xiong, H. Wan, D. Liu, F. Ye, H. Liu, L. Li, H. Xu, X. Du, B. Kang, and X. Zeng. 2016. Insulin stimulates goose liver cell growth by activating PI3K-AKT-mTOR signal pathway. *Cell. Physiol. Biochem.* 38:558–570.

Ho, S. S. C., J. I. Keenan, and A. S. Day. 2020. The role of gastrointestinal-related fatty acid-binding proteins as biomarkers in gastrointestinal diseases. *Dig. Dis. Sci.* 65:376–390.

Kawasaki, T., K. Igarashi, T. Koeda, K. Sugimoto, K. Nakagawa, S. Hayashi, R. Yamaji, H. Inui, T. Fukusato, and T. Yamanouchi. 2009. Rats fed fructose-enriched diets have characteristics of nonalcoholic hepatic steatosis. *J. Nutr.* 139:2067–2071.

Le, M. T., R. F. Frye, C. J. Rivard, J. Cheng, K. K. McFann, M. S. Segal, R. J. Johnson, and J. A. Johnson. 2012. Effects of high-fructose corn syrup and sucrose on the pharmacokinetics of fructose and acute metabolic and hemodynamic responses in healthy subjects. *Metab. Clin. Exp.* 61:641–651.

Lin, W.-T., T.-F. Chan, H.-L. Huang, C.-Y. Lee, S. Tsai, P.-W. Wu, Y.-C. Yang, T.-N. Wang, and C.-H. Lee. 2016. Fructose-rich beverage intake and central adiposity, uric acid, and pediatric insulin resistance. *J. Pediatr.* 171:90.

Liu, L., X. Zhao, Q. Wang, X. X. Sun, L. L. Xia, Q. Q. Wang, B. Yang, Y. H. Zhang, S. Montgomery, H. Meng, T. Y. Geng, and D. Q. Gong. 2016. Prosteatotic and protective components in a unique model of fatty liver: gut microbiota and suppressed complement system. *Sci. Rep.* 6:31763, doi:10.1038/srep31763.

Liu, Y., J. Wang, S. Luo, Y. Zhan, and Q. Lu. 2020. The roles of PPAR gamma and its agonists in autoimmune diseases: a comprehensive review. *J. Autoimmun.* 113:102510, doi:10.1016/j.jaut.2020.102510.

Livak, K. J., and T. D. Schmittgen. 2001. Analysis of relative gene expression data using real-time quantitative PCR and the 2⁻(Delta Delta C(T)) method. *Methods (San Diego, Calif.)* 25:402–408.

Molette, C., P. Berzaghi, A. D. Zotte, H. Remignon, and R. Babile. 2001. The use of near-infrared reflectance spectroscopy in the prediction of the chemical composition of goose fatty liver. *Poult. Sci.* 80:1625–1629.

Montgomery, M. K., C. E. Fiveash, J. P. Braude, B. Osborne, S. H. J. Brown, T. W. Mitchell, and N. Turner. 2015. Disparate metabolic response to fructose feeding between different mouse strains. *Sci Rep.* 5:18474, doi:10.1038/srep18474.

Neuschwander-Tetri, B. A. 2013. Carbohydrate intake and nonalcoholic fatty liver disease. *Curr. Opin. Clin. Nutr. Metab. Care.* 16:446–452.

Pereira, C., M. B. Smolka, R. S. Weiss, and M. A. Brieno-Enriquez. 2020. ATR signaling in mammalian meiosis: from upstream scaffolds to downstream signaling. *Environ. Mol. Mutagen.* 61:752–766.

Pickens, M. K., H. Ogata, R. K. Soon, J. P. Grenert, and J. J. Maher. 2010. Dietary fructose exacerbates hepatocellular injury when incorporated into a methionine-choline-deficient diet. *Liver Int.* 30:1229–1239.

- Rao, C. V., H. Y. Yamada, Y. Yao, and W. Dai. 2009. Enhanced genomic instabilities caused by deregulated microtubule dynamics and chromosome segregation: a perspective from genetic studies in mice. *Carcinogenesis*. 30:1469–1474.
- Roncal-Jimenez, C. A., M. A. Lanaspá, C. J. Rivard, T. Nakagawa, L. Gabriela Sanchez-Lozada, D. Jalal, A. Andres-Hernando, K. Tanabe, M. Madero, N. Li, C. Cicerchi, K. Mc Fann, Y. Y. Sautin, and R. J. Johnson. 2011. Sucrose induces fatty liver and pancreatic inflammation in male breeder rats independent of excess energy intake. *Metab. Clin. Exp.* 60:1259–1270.
- Schwartz, E. A., W.-Y. Zhang, S. K. Karnik, S. Borwege, V. R. Anand, P. S. Laine, Y. Su, and P. D. Reaven. 2010. Nutrient modification of the innate immune response a novel mechanism by which saturated fatty acids greatly amplify monocyte inflammation. *Arterioscler. Thromb. Vasc. Biol.* 30:802–U372.
- Seglen, P. O. 1976. Preparation of isolated rat liver cells. *Methods Cell Biol* 13:29–83.
- Sevastianova, K., A. Santos, A. Kotronen, A. Hakkarainen, J. Makkonen, K. Silander, M. Peltonen, S. Romeo, J. Lundbom, N. Lundbom, V. M. Olkkonen, H. Gylling, B. A. Fielding, A. Rissanen, and H. Yki-Jarvinen. 2012. Effect of short-term carbohydrate overfeeding and long-term weight loss on liver fat in overweight humans. *Am. J. Clin. Nutr.* 96:727–734.
- Siddiqui, R. A., Z. Xu, K. A. Harvey, T. M. Pavlina, M. J. Becker, and G. P. Zaloga. 2015. Comparative study of the modulation of fructose/sucrose-induced hepatic steatosis by mixed lipid formulations varying in unsaturated fatty acid content. *Nutr. Metab.* 12:41, doi:10.1186/s12986-015-0038-x.
- Song, G.-Y., L.-P. Ren, S.-C. Chen, C. Wang, N. Liu, L.-M. Wei, F. Li, W. Sun, L.-B. Peng, and Y. Tang. 2012. Similar changes in muscle lipid metabolism are induced by chronic high-fructose feeding and high-fat feeding in C57BL/J6 mice. *Clin. Exp. Pharmacol. Physiol.* 39:1011–1018.
- Su, S., Y. Wang, C. Chen, M. Suh, M. Azain, and W. K. Kim. 2020. Fatty acid composition and regulatory gene expression in late-term embryos of ACRB and COBB broilers. *Front. Vet. Sci.* 7:317, doi:10.3389/fvets.2020.00317.
- Tang, J. W., M. X. Lu, Q. Q. Fang, F. Z. Lu, R. Y. Shao, J. D. Shen, D. L. Lu, J. He, L. Z. Lu, and D. Niu. 2018. Effects of hydrated sodium calcium aluminosilicate on growth performance, fatty liver, intestine morphology, and serum parameters of overfed geese. *Anim. Prod. Sci.* 58:1876–1884.
- Todoric, J., G. Di Caro, S. Reibe, D. C. Henstridge, C. R. Green, A. Vrbanac, F. Ceteci, C. Conche, R. McNulty, S. Shalpour, K. Taniguchi, P. J. Meikle, J. D. Watrous, R. Moranchel, M. Najhawan, M. Jain, X. Liu, T. Kisseleva, M. T. Diaz-Meco, J. Moscat, R. Knight, F. R. Greten, L. F. Lau, C. M. Metallo, M. A. Febbraio, and M. Karin. 2020. Fructose stimulated de novo lipogenesis is promoted by inflammation. *Nat. Metab.* 2:1034.
- Undamatla, R., L. R. Edmunds, B. Xie, A. Mills, I. J. Sipula, S. P. Monga, and M. J. Jurczak. 2020. Reduced hepatic expression of the mitochondrial quality control factor PARKIN hastens the progression of NAFLD in mice and is associated with NASH in patients. *Diabetes*. 69.
- Vos, M. B., and J. E. Lavine. 2013. Dietary fructose in nonalcoholic fatty liver disease. *Hepatology*. 57:2525–2531.
- Wang, C., L. Jiang, S. Wang, H. Shi, J. Wang, R. Wang, Y. Li, Y. Dou, Y. Liu, G. Hou, Y. Ke, and H. Liu. 2015. The antitumor activity of the novel compound jesridonin on human esophageal carcinoma cells. *Plos One*. 10:118–124.
- Wang, L., B. Waltenberger, E.-M. Pferschy-Wenzig, M. Blunder, X. Liu, C. Malainer, T. Blazevic, S. Schwaiger, J. M. Rollinger, E. H. Heiss, D. Schuster, B. Kopp, R. Bauer, H. Stuppner, V. M. Dirsch, and A. G. Atanasov. 2014. Natural product agonists of peroxisome proliferator-activated receptor gamma (PPAR-gamma): a review. *Biochem. Pharmacol.* 92:73–89.
- Wei, R., C. Han, D. Deng, F. Ye, X. Gan, H. Liu, L. Li, H. Xu, and S. Wei. 2021. Research progress into the physiological changes in metabolic pathways in waterfowl with hepatic steatosis. *Br. Poult. Sci.* 62:118–124.
- Wei, R. X., Q. Song, S. Q. Hu, H. Y. Xu, H. H. Liu, B. Kang, L. Li, X. Y. Zeng, L. Chen, and C. C. Han. 2020. Overfeeding in fluence on antioxidant capacity of serum, liver, gut, and breast muscle in Gang Goose and Tianfu Meat Goose. *J. Appl. Poult. Res.* 29:455–464.
- Wei, S., C. Han, F. He, Q. Song, B. Kang, H. Liu, L. Li, H. Xu, and X. Zeng. 2017. Inhibition of PI3K-Akt-mTOR signal pathway dismissed the stimulation of glucose on goose liver cell growth. *J. Anim. Physiol. Anim. Nutr.* 101:e133–e143.
- Wei, Y., D. Wang, F. Topczewski, and M. J. Pagliassotti. 2007. Fructose-mediated stress signaling in the liver: implications for hepatic insulin resistance. *J. Nutr. Biochem.* 18:1–9.
- Winston, N. 2001. Regulation of early embryo development: functional redundancy between cyclin subtypes. *Reprod. Fertil. Dev.* 13:59–67.
- Xu, H., A. Diolintzi, and J. Storch. 2019. Fatty acid-binding proteins: functional understanding and diagnostic implications. *Curr. Opin. Clin. Nutr. Metab. Care* 22:407–412.
- Xu, L., Y. Duanmu, G. M. Blake, C. Zhang, Y. Zhang, K. Brown, X. Wang, P. Wang, X. Zhou, M. Zhang, C. Wang, Z. Guo, G. Guglielmi, and X. Cheng. 2018. Validation of goose liver fat measurement by QCT and CSE-MRI with biochemical extraction and pathology as reference. *Eur. Radiol.* 28:2003–2012.
- Zhou, C., P. Wang, L. Lei, Y. Huang, and Y. Wu. 2020. Overexpression of miR-142-5p inhibits the progression of nonalcoholic steatohepatitis by targeting TSLP and inhibiting JAK-STAT signaling pathway. *Aging-Us.* 12:9066–9084.